The Frenkel-Kontorova model

L. M. FLORIA[1,3], C. BAESENS[2] and J. GÓMEZ-GARDEÑES[1,3]

[1] Dpt. of Theory and Simulation of Complex Systems, ICMA, CSIC-Universidad de Zaragoza, E-50009 Zaragoza, Spain
[2] Mathematics Institute, University of Warwick. Coventry CV4 7AL, UK
[3] Instituto de Biocomputación y Física de Sistemas Complejos, and Dpto. de Física de la Materia Condensada, Universidad de Zaragoza, E-50009 Zaragoza, Spain

1 Introduction - Presentation of the model

In the preface to his monograph on the structure of Evolutionary Theory [1], the late professor Stephen Jay Gould attributes to the philosopher Immanuel Kant the following aphorism in Science Philosophy: "Percepts without concepts are blind; concepts without percepts are empty". Using with a bit of freedom these Kantian terms, one would say that a scientific model is a framework (or network) of interrelated concepts and percepts where experts build up scientific consistent explanations of a given set of observations. Good models are those which are both, conceptually *simple* and *universal* in its perceptions. Let us illustrate with examples the meaning of this statement.

The mathematical pendulum, *i.e.* a Newtonian mass point of mass m and (angular) position u, subject to a sinusoidal potential $V(u)$, with

$$\text{energy} = \frac{1}{2}m\dot{u}^2 + V(u), \tag{1}$$

is an archetype of good model. The variety of its applications makes it ubiquitous in Physics. Figure 1 shows the formal equivalence of a mathematical pendulum and the Josephson effect between two superconducting electrodes separated by a thin layer of an insulating material. Here the angular variable φ is the so-called gauge invariant superconducting phase difference

$$\varphi = \theta_1 - \theta_2 - (2\pi/\Phi_0)\int_1^2 A dl \tag{2}$$

where A is the electromagnetic vector potential, $\theta_{1(2)}$ are the phases of the wave function of the superconducting state at each electrode, and Φ_0 is a constant called the flux quantum unit.

A second good example is the Ising model, a familiar model in modern Statistical Mechanics. Approaches based on this model play there a role as

basic as pendulum in General Physics does. The Ising model is a lattice or network of N interconnected two-state ($s_j = \pm 1$) nodal elements interacting with energy $J_{ij}s_is_j$ per link, and N is macroscopically large. The complex singular macroscopic behaviour observed in the so-called critical phenomena, has in this conceptual-perceptual framework a referent of rigorous basic understanding. The simplicity of the two-state (on-off, up-down) nodal element on more or less complex connectivity patterns, pervades current theoretical studies in neural networks. It also permeates recent approaches to biological, social and communication networking studies, where interesting generalizations of the model are often needed. In particular, more general dynamical variables at nodes are clearly required in many interesting issues concerning these applications.

The model of interest here belongs, as the pendulum and Ising model, to that class of scientific models which along the years have provided insightful conceptual tools and perceptions in the rigorous analysis of a wide range of theoretical problems. We refer to this model as the Frenkel-Kontorova (FK) model, though other names are sometimes used in the vaste literature on this model. Nowadays, in Statistical and Nonlinear Physics it plays a basic role with important applications in materials and condensed matter systems as well as in several micro- and nano-scale technologies [2, 3].

The *Standard* FK model can be seen as a one-dimensional lattice of identical pendula oscillating in parallel planes, coupled to nearest neighbors by identical (linear) torsion springs.

Alternatively, viewed as a model for spatially modulated structures in solid state physics, the (more general) FK model is a chain of Newtonian particles in one dimension, connected by springs and placed in a spatially periodic potential which represents, for instance, the interaction with a substrate. The total potential energy of the system is formally [1]

$$H(\{u_i\})) = \sum_i V(u_i) + W(u_i, u_{i+1}), \tag{3}$$

where u_i denotes the position of particle i, V is the (on-site) external potential, and W is the interaction potential between (nearest) neighbors. We shall denote by $h(u_i, u_{i+1})$ the local potential energy at site i:

$$h(u_i, u_{i+1}) = V(u_i) + W(u_i, u_{i+1}). \tag{4}$$

In the Standard FK model, u_i denotes the (one-dimensional) angle variable at site i, and the potential functions have the following forms: $V(u) = \frac{K}{4\pi^2}(1 - \cos 2\pi u)$, and $W(u, u') = \frac{1}{2}(u' - u)^2 - \mu(u' - u)$, where μ denotes the natural length of the springs. More generally, we call here (unforced) *Frenkel-Kontorova models*, the systems for which the local potential V is periodic:

[1] *Formally*, because the sum in (3) typically diverges in the case of an infinite chain.

$V(u+1) = V(u)$, to fix ideas, and the interaction function $W(u,u')$ depends only on the difference $u'-u$, i.e., (abusing notations) $W(u,u') = W(u'-u)$ or $W(\Delta u)$ (using the notation $\Delta u = u'-u$), and furthermore W is a (strictly) convex function, so that $W''(u) > 0$. [2] This convexity property of the interactions turns out to be a crucial ingredient both for the well established (rigorous) theory of equilibria in the thermodynamic (infinite system size) limit, that we will summarize in section 2, and for the dissipative dynamics that we will develop in further sections. Much less general theory is available for the cases in which $W(\Delta u)$ is not a convex function.

Motivated in the 30's and 40's (XX century) by studies on plasticity of solids *i.e.* dynamics and thermodynamics of localized lattice imperfections, the model of coupled pendula or other nonlinear oscillators serves today as the referent name of a streamline in the little history of solid state physics research. Localized elementary excitations under terms as diverse as lattice (or discrete) skyrmions, vortices, fronts, solitons, kinks and breathers have emerged as the most convenient basic descriptors of the ubiquitous complex phenomena associated with the competition of:

- self-focussing effect of the nonlinear (non-quadratic) on-site potential $V(u)$, and
- dispersive effect of coupling between sites.

These are the essential ingredients captured in a simplest (though non trivial) way by the FK model. A good indication of the offsprings vigor of this conceptual-perceptual framework is the recent interest (see [4]), both theoretical and experimental, in the issues of localization and transport in Nonlinear lattices. Among the ample variety of current experimental lines of research with which the model is concerned, we now briefly refer to two motivating examples. The first one comes from superconducting technologies [3] at the microscale (micrometer sized devices) which are based on the above mentioned Josephson effect. The second example deals with the elastic properties at the nanoscale level of the DNA double strand.

1.1 A JJ parallel array

The superconducting circuit sketched in figure (1.e) consists of two parallel superconducting wires with equispaced Josephson junctions (JJ) in between, which are labelled by j. The relevant nodal variables φ_j are the gauge invariant phase differences accross the junctions. The equation for their time evolution is

$$\ddot{\varphi}_j + \Gamma\dot{\varphi}_j + \sin\varphi_j = \lambda(\varphi_{j+1} - 2\varphi_j - \varphi_{j-1}) + i_{ext}, \tag{5}$$

[2] We also assume that V and W are twice differentiable.

[3] These technologies have practical uses in quantum metrology, radiofrequency emission, magnetic field and photo-detection, as well as current attempts to (solid state based) quantum computation devices.

where the parameter λ measures the importance of the induced fields, the damping parameter Γ that of the resistive normal current, and i_{ext} the bias external current. The presence of a magnetic field is felt by the electromagnetic circuit as an imposed average torsion per unit length on each field φ_j. Denoting by f_0 the magnetic flux (in quantum flux units) through a single plaquette, the boundary conditions are given by $\varphi_0 = \varphi_1 - 2\pi f_0$ and $\varphi_{N+1} = \varphi_N + 2\pi f_0$ for the case of open-ended arrays, and $\varphi_{N+1} = \varphi_1 - 2\pi n_k$ and $\varphi_0 = \varphi_N - 2\pi n_k$ for ring arrays. The integer n_k is the number of fluxons trapped in the array.

Equation (5) is easily recognized as describing the dynamics of a 1d chain of damped pendula with torque, coupled by torsion springs. Experiments on parallel JJ arrays and their consistent interpretation based on the dynamics of the FK model were reported in [5]. More recently, several designed (periodically inhomogeneous) parallel JJ arrays were experimentally studied showing ratchet transport of fluxon matter, as theoretically predicted [6]. Using the basic tools and concepts from the rigorous theory of FK models, we will show in section 5 that some classes of parametrically driven FK models exhibit collective (non-thermal) ratchet transport.

1.2 Unzipping DNA

Replication and transcription are two basic functions performed by the DNA molecule both inside living cells and in laboratory routine essays. These functions require the opening of base pairs (A-T, G-C, ...) as schematically illustrated in figure (2). Motivated by the possible role of bubble opening in thermal denaturation of double stranded DNA chains, the model of Peyrard-Bishop-Dauxois, PBD for short, tries to capture in a workable simple way the local energy balance which governs the physics of base pair opening.

The relevant variable y_j at pair j is the interbase distance, so that pair opening means "big y". Following the intermolecular potential theory, the following functional form for the on-site potential energy has the appropriate shape:

$$V(y) = D\left(e^{-ay} - 1\right)^2, \tag{6}$$

while the coupling through the double strand of sugar backbone can be assumed either quadratic, as in the original version [7], or sensibly corrected as in [8]:

$$W(y_j, y_{j+1}) = \frac{1}{2}C(y_{j+1} - y_j)^2\left(1 + \rho e^{-\alpha(y_{j+1}+y_j)}\right). \tag{7}$$

The PBD model is a generalized[4] FK model for the elasto-plastic properties of DNA base pair opening. Interesting experiments on DNA unzipping have been already reported [9]. One should note that there is no periodicity symmetry in real DNA of living cells, though periodic blocks in the "junk" cromosomal DNA are well known to be overabundant[10]. Thus the lack of

[4] *generalized*, in the sense that the on-site potential $V(y)$ is not periodic.

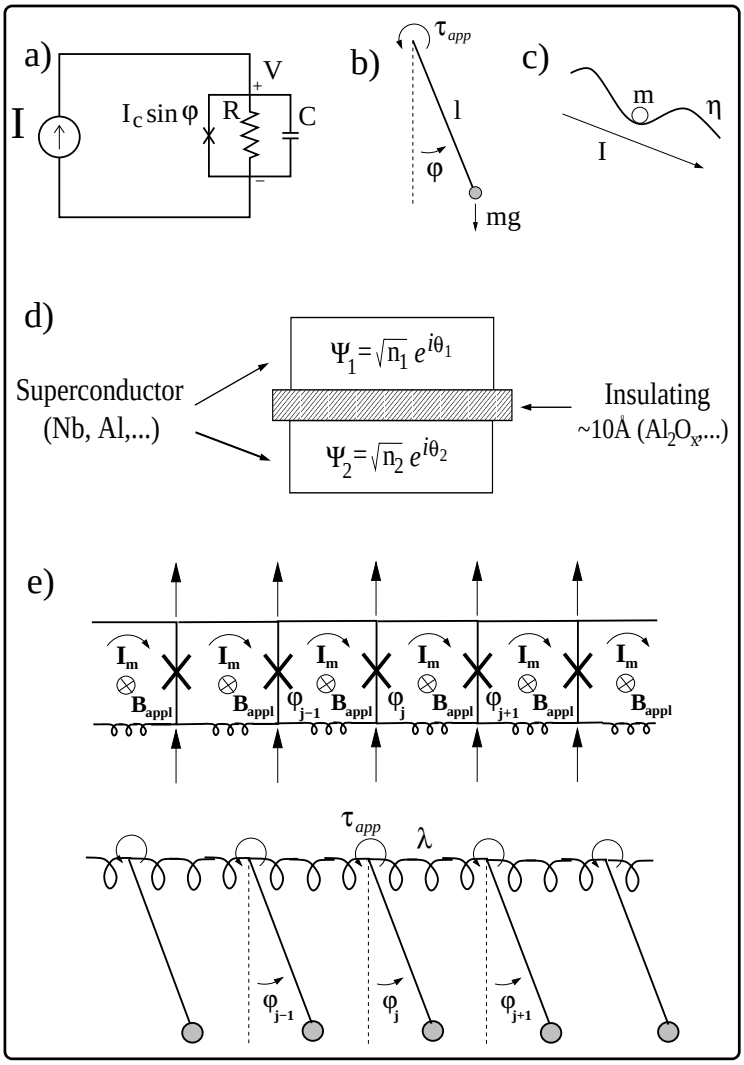

Fig. 1. Equivalence of Josephson junction arrays and chains of coupled pendula. The Josephson current and voltage between the two superconductors of the Josephson junction represented in **(d)** are functions of the phase difference φ introduced in equation (2): $I_J = I_c \sin\varphi$ and $V = \hbar/2e\ d\varphi/dt$. The RCSJ model sketched in **(a)** describes all the contributions for the current in the Josephson junction: $I = I_J + I_R + I_C$. Using the φ-dependence of the voltage and the Josephson current and after normalizing, the equation for the currents becomes $i_{ext} = \ddot{\varphi} + \Gamma\dot{\varphi} + \sin\varphi$. This equation has the same functional form as the one describing the motion of a damped pendulum with torque **(b)** or of a particle in a tilted washboard potential **(c)**. The expression of the single Josephson junction is used for the description of the Josephson junction parallel array **(e)** to obtain equation (5) which, in this case, is formally equivalent to the equation describing the dynamics of a chain of damped pendula with torque (τ_{app}) coupled by torsion springs.

homogeneity is essential for the basic description of many observed phenomena in living double stranded DNA molecules. We stress this point here, as an example of the added complexity in this particular use of the FK model in DNA prospective technologies.

2 Equilibrium states

In condensed matter, a physical motivation for studying equilibrium states of the FK model came from the observed abundance of modulated (structured) phases in minerals as well as in man-made materials and/or compounds, and the need to understand the peculiar multiphase diagrams shown by experiments.

We shall consider here the thermodynamic limit, so equilibrium configurations (or states) will be represented by doubly infinite sequences (u_i), $-\infty < i < +\infty$. Balance of forces at each site n yields[5]

$$0 = -\frac{\partial H}{\partial u_n} = -\frac{\partial (h(u_{n-1}, u_n) + h(u_n, u_{n+1}))}{\partial u_n} \tag{8}$$

$$= W'(u_{n+1} - u_n) - W'(u_n - u_{n-1}) - V'(u_n) \tag{9}$$

for the (general) FK model, and more specifically for the Standard FK model

$$u_{n+1} - 2u_n + u_{n-1} - \frac{K}{2\pi} \sin 2\pi u_n = 0 \tag{10}$$

There is a one-to-one correspondence between equilibrium configurations (u_n) of an FK model and orbits $((u_n, p_n))$ of a symplectic twist map of the cylinder, which can be obtained from (9) using a Legendre transform, as usually done to go from the Lagrangian formulation of a problem to the Hamiltonian one. Setting $p_n = -\frac{\partial h(u_n, u_{n+1})}{\partial u_n} = W'(u_{n+1} - u_n) - V'(u_n)$, the convexity condition $W'' > 0$ allows to invert this expression to obtain u_{n+1} as a function of u_n and p_n, and then we use $p_{n+1} = W'(u_{n+1} - u_n)$. For instance, for the Standard FK model, we easily obtain from (10):

$$u_{n+1} = u_n + p_n + \frac{K}{2\pi} \sin 2\pi u_n \tag{11}$$

$$p_{n+1} = p_n + \frac{K}{2\pi} \sin 2\pi u_n \,, \tag{12}$$

This is the familiar Standard map, paradigm example of a twist map[6] of the cylinder.

---

[5] Though the energy H in (3) may be infinite, its gradient is well defined.

[6] *twist* means that $\frac{\partial u_{n+1}}{\partial p_n} > 0$, and this is equivalent to the convexity condition on W.

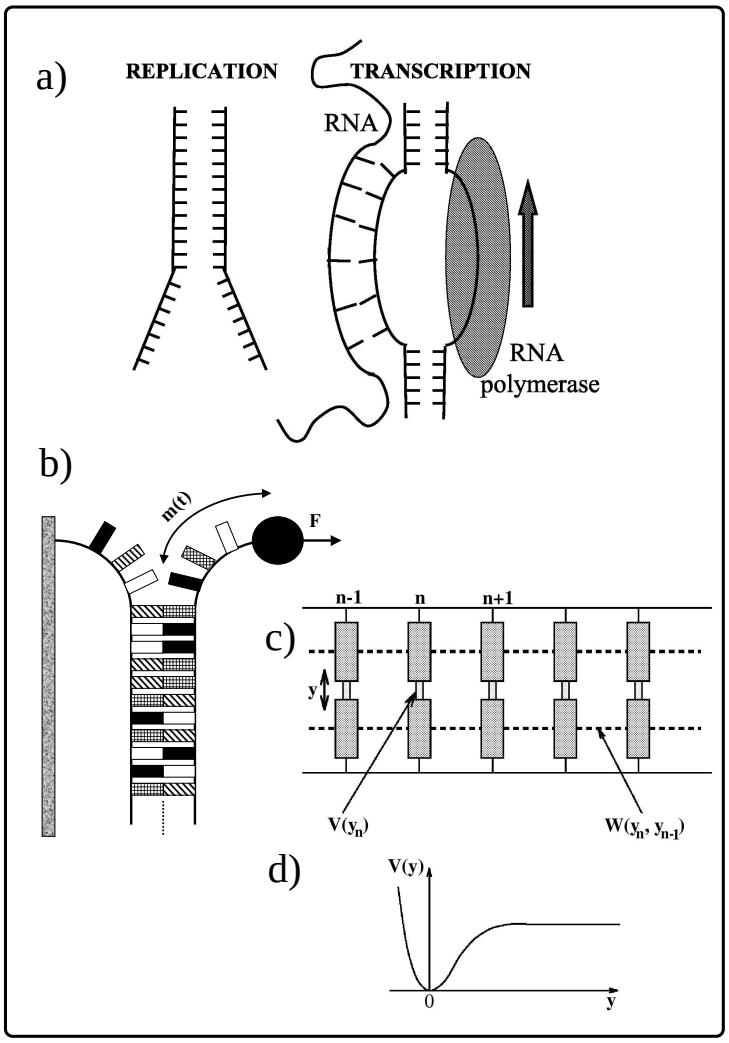

Fig. 2. **(a)** Schematic representation of the Replication and Transcription of the DNA. The DNA unzipping involved in the two processes is described using a constant force scheme based on the Peyrard-Bishop-Dauxois sequence dependent model, as sketched in **(b)**. In the PBD model, sketched in **(c)**, the relevant on-site variable is the distance y_j between the two bases of the pair j. The potential $V(y_j)$ accounts for the interaction between these two nucleotides (A-T or G-C), and $W(y_j, y_{j+1})$ is the energy of interaction between neighboring pairs j and $j+1$. **(d)** Shape of the potential $V(y)$ given by equation (6).

Of particular importance are the *minimum energy configurations*, m.e.c. for short, which are sequences (u_j) such that, given any integers $m < n$,

$$H_{mn} \equiv \sum_{j=m}^{n-1} h(u_j, u_{j+1}) \tag{13}$$

is (globally) minimal with respect to all variations of $(u_{m+1}, \ldots, u_{n-1})$, keeping u_m and u_n fixed. They correspond to action-minimizing orbits of the associated twist map.

M.e.c. are also local minima of the energy (3), meaning equilibrium configurations for which the quadratic form in the series expansion of the energy around the equilibrium is positive or zero:

$$\delta H \simeq \frac{1}{2} \sum_{m,n} \frac{\partial^2 H}{\partial u_n \partial u_m} \delta_n \delta_m \geq 0 \tag{14}$$

(for square summable (δ_n)). Local minima are (linearly) stable equilibria. For stable equilibria, the eigenvalues of the linear stability matrix $(\partial^2 H/\partial u^2)_{mn}$ are non-negative; these are the squared eigenfrequencies of small oscillations around the equilibrium (u_j). Together with their limit points, they form the *phonon spectrum* of the configuration. The presence of a gap Δ_{ph} in the phonon spectrum, meaning the spectrum is bounded away from zero, reflects the breaking of continuous translational invariance in the lattice state.

Because $h(u, u')$ does not depend on the index (lattice homogeneity) and it is (diagonally) periodic: $h(u+1, u'+1) = h(u, u')$, the action of the group of translations $\{\sigma_{rm} : r, m \text{ integers}\}$ on configurations (u_j), defined by

$$\sigma_{rm}(u_j) = (u_{j+r} + m), \tag{15}$$

preserves the equilibrium property and the minimum energy property.

Given two configurations (u_j), (v_j), one says that the first one is less than the other $(u_j) < (v_j)$ if $u_j < v_j$ for all j. A configuration is *rotationally ordered*, RO for short, if the set of its translates by all the σ_{rm} is a totally ordered set of configurations. It follows that a RO configuration (u_n) has a well defined mean spacing between particles (or torsion angle between pendula)

$$\langle u_{n+1} - u_n \rangle = \lim_{n \to \infty, m \to -\infty} \frac{u_n - u_m}{n - m} = \omega \tag{16}$$

and furthermore satisfies

$$|u_{n+r} - u_n - r\omega| < 1 \qquad \text{for all integers } r, n. \tag{17}$$

This quite constraining RO property is particularly important, as it turns out that

$$\text{m.e.c.} \Rightarrow \text{RO}. \tag{18}$$

Indeed, since the interaction potential $W(\Delta u)$ is convex, it costs less energy for configurations to differ as little as possible (given the potential $V(u)$) from equispaced configurations with same mean spacing, *i.e.* to be RO.

Macroscopic variables are averages over the lattice state, which can be computed with the appropriate distribution functions. For RO configurations, these are the distribution functions (modulo 1), d.f. (mod 1) for short, of real doubly infinite sequences:
Let us denote by $F_{\mathbf{u}}^{M,N}(x)$ the fraction of indices n, $(M \leq n \leq N)$, for which the fractional part $\mathrm{Frac}(u_n)$ lies in the interval $[0, x)$. The distribution function (mod. 1) $F_{\mathbf{u}}(x)$ of the configuration $\mathbf{u} = (u_j)$, $(0 \leq x \leq 1)$, is defined as the limit

$$F_{\mathbf{u}}(x) = \lim_{M \to -\infty, N \to \infty} F_{\mathbf{u}}^{M,N}(x) \tag{19}$$

provided the limit exists. Clearly, $F_{\mathbf{u}}(x)$ is a non-decreasing function, with $F(0) = 0$ and $F(1) = 1$. Not every conceivable sequence possesses it, but RO configurations do. Thus, quantities like the mean spacing or the mean energy per particle $\epsilon = \langle h(u_n, u_{n+1}) \rangle$ of RO configurations can be computed as the Stieltjes integrals

$$\omega = \int_0^1 \Delta u \; dF_{\mathbf{u}} \tag{20}$$

$$\epsilon = \int_0^1 h(u, u') \; dF_{\mathbf{u}} \tag{21}$$

where $F_{\mathbf{u}}$ is the d.f. of the configuration (u_j). [7] The d.f. (mod 1) of a RO configuration may either have plateaux at intervals where no particles locate (modulo 1), and jumps, or be a smooth function in some other instances.

For every mean spacing there is at least one recurrent m.e.c. (called *ground state*) [11]. This property (recurrent) means that given any integer r and any number $\epsilon > 0$, there are integers m and $s > 0$ such that both inequalities $|u_{r+s} - u_r - m| < \epsilon$ and $|u_{r+s+1} - u_{r+1} - m| < \epsilon$ are satisfied. Recurrent configurations of the FK model correspond to recurrent orbits of the associated twist map. The distribution function (mod 1) F_ω of a ground state defines a whole class of equivalent ground states as follows: take an arbitrary real α, and consider $f = F_\omega^{-1}$ (the inverse of F_ω) and lift it to the real line by $f(u + 1) = f(u) + 1$; then the configuration $(u_n) = (f(n\omega + \alpha))$ is a ground state equivalent to the original one.

Commensurate ground states (u_n) are (spacially) periodic (of minimal period), in the sense that they satisfy a relation of the form $u_{n+q} = u_n + p$ for all n, where $q > 0$ and p are coprime integers, and so their mean spacing is the rational number $\omega = p/q$. These configurations are generically *pinned*, meaning that one has to put some finite energy E_{PN} on the system to displace the

[7] In what follows, we will drop the suffix $\mathbf{u}$ when it is clear which configuration we are talking about, or we may use the suffix ω to emphasize that it is the d.f. (mod 1) of a configuration with mean spacing ω.

configuration over the path-dependent barriers of energy (Peierls-Nabarro barriers) separating configurations that are equivalent up to translations σ_{mn}[8]. The value of E_{PN} is the energy difference between the ground state and a RO minimax (unstable equilibrium) configuration (the saddle point configuration) ordered between two contiguous ground states.

A pinned configuration has a finite *coherence length* (or *decay range*) of fluctuations, ξ, meaning that if a field component, say u_{n_0}, is externally displaced, this produces displacements of the other components u_n, which decay exponentially with the distance $|n - n_0|$: $\sim \exp(-|n - n_0|/\xi)$. Also, there is a gap $\Delta_{ph} > 0$ in the phonon spectrum.

Ground states with irrational mean spacing ω, called *incommensurate*, can be viewed as limits of sequences of periodic configurations of mean spacing $p_n/q_n \to \omega$ as $n \to \infty$. The physical properties of these structures depend on the parameter K of the model: for each irrational ω there is a critical value $K_c(\omega)$ of K s.t.

- for $K < K_c$ the d.f. (mod 1) is a continuously differentiable strictly increasing function: the family of ground states form a continuum and correspond to the orbits of an invariant Kolmogorov-Arnold-Moser torus for the twist map of the cylinder. The ground state is sliding (unpinned), so that $E_{PN} = 0$. Consequently, localized induced fluctuations extend through the lattice and the decay range diverges: $\xi \to \infty$. The phonon spectrum is gapless.
- For $K > K_c$ the d.f. (mod 1) becomes the inverse of a so-called Cantor function and the family of ground states form a Cantor set (called Aubry-Mather set, or cantorus in the twist map context). They are pinned: $E_{PN} > 0$, $\Delta_{ph} > 0$, and ξ has a finite value. The transition at $K_c(\omega)$ corresponds to the breaking of the invariant KAM torus into a cantorus, and the fractalization of such continuous invariant sets is a critical phenomenon [12, 13].

Besides the ground states, there are non-recurrent m.e.c. called discommensurations, DC for short. These configurations connect asymptotically ($n \to \pm\infty$) two contiguous commensurate ground states (typically one is a translate of the other, but they can be different in general) by an energy minimizing path of exponentially localized length (the width of the DC) around a lattice site (the center of the DC). They correspond to heteroclinic orbits of the associated area-preserving twist map. The width of the DC is given by the decay range ξ of the recurrent asymptotic configuration. Note also that the d.f. (mod 1) of a DC coincides with that of the recurrent substrate (the deviation of a DC configuration relative to substrate being exponentially localized).

The DCs are elementary defects, *i.e.*, localized compressions (retarded DCs) or expansions (advanced DCs) superimposed on the recurrent substrate

[8]We assume here that there is only one ground state up to translations σ_{mn}

modulation. If ω is close to a rational $\omega_0 = p/q$, the ground state with mean spacing ω can be viewed as an "array of DCs" (advanced if $\omega > \omega_0$, retarded if $\omega < \omega_0$) over the recurrent (periodic) ground state of mean spacing ω_0. The interaction energy between neighboring DCs decays exponentially with the quotient interdistance/width, $\sim \exp(-1/(\xi|\omega - \omega_0|))$, so that for ω very close to ω_0 and/or high values of K (*i.e.* ξ small), these elementary localized excitations are almost non-interacting (and pinned).

We call Discommensuration Theory the theoretical perspective which describes the modulated phase as a system of localized DCs (weakly, or not so weakly) interacting. Note that it is a description built upon an emergent property which assumes the role of new elementary component of the many-body system, roughly illustrating the notion of *emergent* property in Complex Systems theory [14, 15] [9].

There are two limits in which the equilibrium states of a Frenkel-Kontorova model can be found explicitly.
(i) If $K = 0$ (i.e. no external potential), called the *the integrable limit*, then the equation for equilibria reduces to

$$-W'(u_{n+1} - u_n) + W'(u_n - u_{n-1}) = 0 \qquad \text{for all } n, \tag{22}$$

that is, the terms $W'(u_{n+1} - u_n)$ are the same for all n. Now the function W' is strictly increasing since $W'' > 0$ (convexity condition), so it follows that for all n, the difference$u_{n+1} - u_n = u_n - u_{n-1}$ is a constant independent of n, equal to ω, say. Hence equilibria are configurations of the form

$$u_n = n\omega + \alpha \qquad \forall n \tag{23}$$

where α is some constant. So, for every value ω of the mean spacing, there is a one-parameter family (continuum) of equispaced equilibria, parametrized by the phase α.
(ii) If $W(u) \equiv 0$ (i.e. no interaction between neighbors), called the *anti-integrable limit*, then the equation for equilibria reduces to

$$-\frac{\partial H}{\partial u_n} = -V'(u_n) = 0 \qquad \forall n \tag{24}$$

It follows that any sequence of critical points of the potential V is an equilibrium state. For instance, for the Standard FK model, $V'(u_n) = K/2\pi \sin 2\pi u_n = 0$ so any sequence of half-integers is an (anti-integrable) equilibrium state: there are lots of them!

Sequences (u_n) of minima of V are local minima of the total energy and correspond to metastable states. Minimum energy configurations are now only *weakly* rotationally ordered (meaning that translates by the σ_{rm} may touch: $(\sigma_{r,m}\boldsymbol{u})_j \leq u_j$ (or $\geq u_j$) for all j, instead of strict inequalities). In the case

[9] Temperature, however, is the archetype among the simplest examples, being much richer and deeper.

where $V(u)$ has a unique minimum per period, at $u = a$, say, it is easy to see that the ground states of mean spacing ω are of the form

$$u_n = \mathrm{Int}(n\omega + \alpha) + a \qquad \forall n \tag{25}$$

where α is a constant. Obviously, this one-parameter family of ground states does not form a continuum like in the integrable limit.

We will use these two limits for our models of collective ratchet transport in further sections.

For a more extensive (and mathematically oriented) presentation of the theory of equilibrium states of FK, we refer to [16]; the Aubry-Mather theory of minimum energy states can also be found in [17] and [18].

3 Dissipative dynamics

Non-equilibrium situations in the framework of the FK model are certainly of interest concerning many theoretical and experimental studies. In particular, the behaviour of Hamiltonian nonlinear discrete fields is of fundamental interest in Theoretical Physics. However, in connection to experimental and prospective technological research, two ingredients are often important to add to the ideal Hamiltonian description:

- Coupling to other (external) variables are often amenable to an analysis in terms of driven and damped dynamics and/or
- Thermal effects (Langevin, or other dynamics).

Even neglecting thermal effects (noise), a full characterization of the lattice dynamics governed by equations of the form

$$m\ddot{u}_n + \Gamma\dot{u}_n = C(t)(\Delta^2 u)_n + K(t)V'(u_n) + \mathcal{F}(t) \tag{26}$$

where $(\Delta^2 u)_n$ denotes the dicrete Laplacian $u_{n+1} - 2u_n + u_{n-1}$ is a formidable task, with too many interesting aspects, which is well beyond the scope of these lectures. We shall restrict here to a particular regime of parameters, the *overdamped* [10] (or *dissipative*) limit $m/\Gamma \to 0$, *i.e.* we shall drop the inertial term $m\ddot{u}_n$ in (26) and consider systems of the form

$$\dot{u}_n = C(t)(\Delta^2 u)_n + K(t)V'(u_n) + \mathcal{F}(t) \tag{27}$$

for which the dynamics are relatively simple due to the following property of (27): if two initial conditions are ordered, their trajectories will remain so at any later time:

[10] This limit is called *gradient dynamics* in the lectures by C. Baesens. Indeed the right hand side in (27) is the gradient of the total energy H. In those lectures, overdamped means inertial dynamics (26) with ratio m/Γ small enough but not zero.

$$(u_i(0)) < (v_i(0)) \Rightarrow (u_i(t)) < (v_i(t)) \quad \text{for all } t > 0, \tag{28}$$

i.e., the dynamics of the *overdamped* system preserve the (partial) order on sequences [19, 20, 21, 18]. This order-preserving property originates from the convexity of the interaction potential $W(\Delta u)$.

Since the set of translates $\{\sigma_{r,n}(u_j)\}$ of an RO configuration (u_j) is a totally ordered set, we deduce that the RO property is preserved under the dynamics of (27). Given the key role played by rotational order in the theory of m.e. equilibrium states, one may wonder if it can be of use in the analysis of the dynamics of (27). The answer, as will be seen in the lectures by C. Baesens on monotone dynamics, is positive. The dynamics of RO configurations is easier to characterize (the d.f. (modulo 1) $F_{(\tilde{u}_j)}(x;t)$ is well defined and it carries over all the information on the configuration $(\tilde{u}_j(t))$, if it is recurrent). Even more, a RO trajectory $(\tilde{u}_j(t))$ and its translates $\sigma_{r,m}(\tilde{u}_j(t))$ (associated to the same d.f.(mod 1) $F_{(\tilde{u}_j)}(x;t)$) can be used, like a fisher net, to bound (finite spacing) trajectories $(u_j(t))$ that have same mean spacing:

$$\sigma_{r_1,m_1}(\tilde{u}_j(t)) < (u_j(t)) < \sigma_{r_2,m_2}(\tilde{u}_j(t)). \tag{29}$$

This sandwich construction plays a central role in proving, for instance, uniqueness (for initial conditions with bounded spacing and a same mean spacing) of the asymptotic average velocity (or flow) of the chain:

$$\mathcal{J} = \lim_{T\to\infty} T^{-1} \int_0^T \langle \dot{u}_n \rangle \, dt \tag{30}$$

Extensive numerical studies have motivated (and guided in some cases) rigorous results and theorems in this field. We now highlight some remarkable features of the dynamics of (27) revealed by numerics [20].

1. *Existence of thresholds for transport.* A kind of ubiquitous peculiarity in many observed transport phenomena is the existence of threshold values of the drive parameter, below which equilibrium is stable and no transport occurs. The characterization of thresholds for both cases of additive and parametric driving can be done. For example, under constant additive force $\mathcal{F}(t) = \mathcal{F}$ (and constant parameters K and C) there is a mean spacing dependent depinning force $\mathcal{F}_{th}(\omega) > 0$ if K is large enough, beyond which the structure slides and the asymptotic state is unique [21]. The scaling of different quantities at the depinning transition is nontrivial for irrational values of ω. The issue of thresholds for parametric driving ($\mathcal{F}(t) \equiv 0$, $K(t)$ or $C(t)$ not constant in (27)) will be addressed in the section 6 for a specific model which is amenable to exact analysis.
2. *Multiple attractor coexistence.* The uniqueness of asymptotic sliding states observed for constant additive force does not extend if the additive force is periodic in time. This is also the case for general parametric driving. The abundance of metastable equilibria has its counterpart in the coexistence of multiple resonant (synchronization) states, all sharing the common average velocity value.

3. The addition of a small inertial term $m\ddot{u}_n$ in (26) does not alter qualitatively the dynamics. A preserved partial order has also been found in this case [22].

4 Exercises

1. Distribution functions (mod 1) of the integrable limit configurations.
   (a) Compute the d.f. (mod 1) $\tilde{F}_{\omega,\alpha}(x)$ of the sequence $(\tilde{u}_n) = (n\omega + \alpha)$ for rational $\omega = p/q$ (p and q coprime integers).
   (b) Deduce that for irrational values of ω, $\tilde{F}_{\omega,\alpha}(x) = x$.

2. Use the results of previous exercise to compute the fraction $\mu(\alpha, \beta, \omega)$ of indices n for which $\mathrm{Int}(n\omega + \alpha) \neq \mathrm{Int}(n\omega + \beta)$, for rational and irrational values of ω.

4.1 Solutions to Exercises

1. (a) The sequence $\mathrm{Frac}(np/q + \alpha)$, $-\infty < n < +\infty$, is periodic of period q and takes values $\epsilon + lq^{-1}$, $l = 0 \ldots, q-1$, where $\epsilon = q^{-1}\mathrm{Frac}(q\alpha) < q^{-1}$ for all α. To compute the limit (19) which defines the d.f. (mod 1), we may consider a subsequence of $F^{M,N}_{\tilde{\mathbf{u}}}(x)$ for which $N - M + 1 = qj$ ($j = 1, 2, \ldots$), for fixed α and x. Such a subsequence is clearly constant (independent of j), so one only needs to compute $F^{1,q}_{\tilde{\mathbf{u}}}(x)$, this value giving the limit $\tilde{F}_{p/q,\alpha}(x)$.
   If $\epsilon < x < 1$, then the number of indices n ($1 \leq n \leq q$) such that $\mathrm{Frac}(np/q + \alpha) < x$ is the number of consecutive segments of length q^{-1} inside the interval $[\epsilon, x)$, *i.e.* $1 + \mathrm{Int}(q(x - \epsilon)^-)$, where $\mathrm{Int}(x^-)$ denotes the greater integer less than x (*i.e.* equals the integral part of x, $\mathrm{Int}(x)$, except at integers). This expression gives also the correct (zero) result for $0 \leq x \leq \epsilon$. Using the property $1 + \mathrm{Int}(x) = -\mathrm{Int}((-x)^-)$, one obtains

$$\tilde{F}_{p/q,\alpha}(x) = -q^{-1}\mathrm{Int}(q(-x + q^{-1}\mathrm{Frac}(q\alpha))) \tag{31}$$

   Note that $\tilde{F}_{p/q,\alpha}(x + q^{-1}) = \tilde{F}(x) + q^{-1}$, for $x < 1 - q^{-1}$. Also, the change $\alpha \to \alpha + q^{-1}$ leaves $\tilde{F}_{p/q,\alpha}(x)$ invariant.
   (b) An irrational number ω is the limit of a sequence of rational numbers $p_l/q_l \to \omega$, with $p_l \to \infty$ and $q_l \to \infty$ as $l \to \infty$ (p_l and q_l coprime for each l).
   Thus, using the previous result for each rational approximant p_l/q_l and the fact that $q_l^{-1}\mathrm{Frac}(q_l\alpha) \to 0$ for all α as $l \to \infty$, we obtain

$$\tilde{F}_{\omega,\alpha}(x) = \lim_{l\to\infty} -q_l^{-1}\mathrm{Int}(-q_l x) = x\,, \tag{32}$$

which does not depend on α. In other words, orbits of an irrational rotation are uniformly distributed on the circle . A proof of this well-known result, based on the Weyl criterion, can be found in [23].

2. The fraction $\mu(\alpha,\beta,\omega)$ of indices n for which $\mathrm{Int}(n\omega+\alpha) \neq \mathrm{Int}(n\omega+\beta)$ can be obtained from the distribution functions (mod 1) $\tilde{F}_{\omega,\alpha}(x)$ and $\tilde{F}_{\omega,\beta}(x)$ as follows:
Write $n\omega+\beta = n\omega+\alpha+(\beta-\alpha)$ and split terms between their integral and fractional parts, and then realize that

$$\mathrm{Int}(n\omega+\alpha) = \mathrm{Int}(n\omega+\beta) \tag{33}$$

iff

$$\alpha-\beta \leq \mathrm{Frac}(n\omega+\alpha) < 1+\alpha-\beta \tag{34}$$

or, equivalently, iff

$$\beta-\alpha \leq \mathrm{Frac}(n\omega+\beta) < 1+\beta-\alpha. \tag{35}$$

Thus, the indices n violating (33) are those violating any of the inequalities in (34) or, equivalently, any of the inequalities in (35). There are different cases, depending on $\alpha-\beta$:
(i) For $0 \leq \alpha-\beta < 1$ the second inequality in (34) holds for all n, while the first inequality is violated when $\mathrm{Frac}(n\omega+\alpha) < \alpha-\beta$, so $\mu(\alpha,\beta,\omega) = \tilde{F}_{\omega,\alpha}(\alpha-\beta)$. Alternatively, the first inequality in (35) holds for all n, while the second inequality is violated when $\mathrm{Frac}(n\omega+\beta) \geq 1+\beta-\alpha$, so $\mu(\alpha,\beta,\omega) = 1-\tilde{F}_{\omega,\beta}(1+\beta-\alpha)$.
(ii) For $\alpha-\beta \geq 1$ both inequalities in (34) are violated for all n, so that $\mu(\alpha,\beta,\omega) = 1$.
Hence we obtain

$$\mu(\alpha,\beta,\omega) = \begin{cases} 1 & \text{if } |\alpha-\beta| \geq 1 \\ \tilde{F}_{\omega,\alpha}(\alpha-\beta) = 1-\tilde{F}_{\omega,\beta}(1+\beta-\alpha) & \text{if } 0 \leq \alpha-\beta < 1 \\ \tilde{F}_{\omega,\beta}(\beta-\alpha) = 1-\tilde{F}_{\omega,\alpha}(1+\alpha-\beta) & \text{if } 0 \leq \beta-\alpha < 1 \end{cases} \tag{36}$$

where, for rational $\omega = p/q$, $\tilde{F}_{p/q,\alpha}(x)$ is given by (31), and for irrational ω, $\tilde{F}_{\omega,\alpha}(x) = x$ (equation (32)). Thus, in the irrational case, $\mu(\alpha,\beta,\omega)$ depends only on the difference $x = \alpha-\beta$, and one obtains the piecewise linear function

$$\mu(x) = \begin{cases} 1 & \text{if } x \leq -1 \\ -x & \text{if } -1 < x \leq 0 \\ x & \text{if } 0 \leq x < 1 \\ 1 & \text{if } 1 \leq x\ . \end{cases} \tag{37}$$

5 Ratchet effect

Think of a Brownian particle experiencing a mirror-asymmetric periodic potential $V(u)$, so that the density distribution function $\rho(u)$ (d.d.f. for short) of the particle position u is peaked around the minimum of the potential (see figure 3). Then turn ideally the potential off, so that the d.d.f. diffuses symmetrically and, after a while, turn the potential on again: as shown in figure the distribution centroid (or mean position) $\int u\,\rho(u)\,du$ has been shifted. This directional transport results from the symmetric diffusion of the d.d.f. followed by asymmetric localization. The rectification of thermal fluctuations in asymmetric environments is commonly referred to as *ratchet effect* in recent litterature [24].

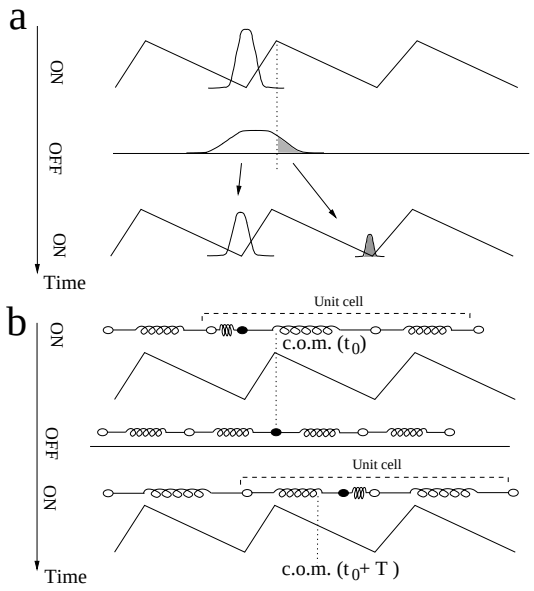

Fig. 3. Thermal versus collective flashing ratchet mechanism. Panel **a** shows schematically the thermal broadening of the density distribution function of one particle when the potential is off and how this can produce directed motion when switched on again. In **b** the collective interaction between particles in an extended system produces again a net flow when switching on and off the asymmetric potential. In both cases the particle mainly responsible for the flow in this cycle has been highlighted. The center of mass of the unit cell (three particles in two periods of the potemtial) at t_0 and $t_0 + T$ is marked by the dotted line to see the one-cycle advance.

A slightly different version of the ratchet effect is the following: instead of turning on-off the potential $V(u)$, we can monitor the temperature so that

the amplitude of the thermal fluctuations (the strength of the diffusive forces) is turned on and off. At zero temperature, the d.d.f. of the particle position is sharply localized at the minimum of the potential, while at high enough temperature, it widens enough to allow ratchet transport when switching temperature on and off cyclically.

Now think of an equilibrium structure of a FK model with a mirror-asymmetric shape for $V(u)$ and turn this potential off, so that only diffusive forces (interaction potential $W(\Delta u)$) act on the lattice. After relaxation to equispaced equilibrium turn the potential $V(u)$ on again. Does one observe transport in this cyclic process? The following unsophisticated argument provides a positive answer to this question (and an estimation of the flow).

- The distribution centroid $u_{cm}(\mathbf{u}) = \int_0^1 x\, dF_{\mathbf{u}}(x)$, of the configuration $\mathbf{u} = (\mathbf{u_n})$, cannot change when the potential $V(u)$ is turned off, due to Newton's third law. To compute the centroid displacement during the on-semicycle, let us denote by $[\Delta, \Delta+1]$ the set of values of the initial position $u_0(0)$ of particle 0 in an equispaced configuration, such that $u_0(\infty)$ (the asymptotic position of the particle after the potential has been turned on again) lies inside the 0^{th} well of the potential $V(u)$ (which we assume to be the interval $[0,1]$). The centroid of the uniform distribution in $[\Delta, \Delta+1]$ is located at $\Delta + 1/2$, while the distribution centroid of the asymptotic equilibrium is $u_{cm}(\mathbf{u}(\infty)) = \int_0^1 x\, dF_{\mathbf{u}(\infty)}(x)$. Thus, the centroid displacement in one cycle is simply $u_{cm}(\mathbf{u}(\infty)) - \Delta - 1/2$. One has just to realize that a zero value for this quantity cannot be generic, but indeed rather exceptional provided the mirror-asymmetry condition on $V(u)$.

This "poor man" derivation can be properly formalized, in order to provide a rigorous proof of existence of collective (non thermal) ratchet effect in FK models, as we will see in the following section.

The "temperature on-off" version of the thermal ratchet effect has also a collective ratchet counterpart in the following (non thermal) cycle: Turn on and off the coupling potential $W(u,u')$ of the FK model. For this version we will also find ratchet transport, provided the coupling parameter is turned on above some threshold value which depends on the mean spacing ω (and the specific potential functions).

For both versions of the collective ratchet effect, the Discommensuration Theory [25] provides deep insights into the details of this transport phenomenon. This will be analyzed in section 7, before concluding with a few exercises in section 8.

6 Collective ratchet effects in FK model

To fix ideas, we shall consider here FK models with harmonic coupling, *i.e.* $W(u,u') = \frac{1}{2}(\Delta u)^2 - \mu \Delta u$, $(\Delta u = u' - u)$, and shall assume that the on-site potential $V(u)$ has a single minimum per period, at $u = a \pmod 1$,

$0 < a < 1$, and maxima at integer values of u. More specifically, in the first version of the collective FK ratchet, we will denote by K the amplitude of the on-site potential and write $K\,V(u)$ instead of $V(u)$. For the second version, this amplitude will be kept equal to unity, and we will parametrize the interaction, writing $C\,W(\Delta u)$, instead of $W(\Delta u)$, where C $(= K^{-1})$ is the coupling parameter.

In version 1 (respectively 2), $K(t)$ (resp. $C(t)$) will be a crenelated function of time, taking alternatively values 0 and K (resp. 0 and C), for times of length $\tau_{\rm off}$ and $\tau_{\rm on}$ respectively, so that the period of a cycle is $T = \tau_{\rm off} + \tau_{\rm on}$. Both semiperiods $\tau_{\rm off}$ and $\tau_{\rm on}$ are assumed to be much larger than the characteristic times of relaxation to equilibrium. This last assumption allows to impose equilibrium conditions on configurations at switching times. We also assume the overdamped limit of dynamics:

$$\dot{u}_n = (\Delta^2 u)_n + K(t)\,V'(u_n) \quad \text{(version 1)} \tag{38}$$

$$\dot{u}_n = C(t)\,(\Delta^2 u)_n + V'(u_n) \quad \text{(version 2)} \tag{39}$$

Under the overdamped dynamics, rotational order and mean spacing are preserved, and we have uniqueness of the asymptotic average velocity (or flow, (30)) for fixed mean spacing; also ground states are RO. These facts will allows us to restrict our analysis to RO configurations for which distribution functions (mod 1) are defined. The algorithm to compute the flow, or equivalently, the displacement of the distribution centroid during a cycle, will be to count the fraction of particles that pass over the position $u = 0$ (mod 1) during each semicycle, $\mathcal{J}^0_{\rm off}$ and $\mathcal{J}^0_{\rm on}$ and add them up.

6.1 Switching potential $V(u)$ on-off

The initial configuration (before turning the potential off) at $t = 0$ is assumed to be a ground state (i.e., a recurrent and minimum energy configuration) of mean spacing ω for the value K of the potential amplitude. Its d.f. (mod 1) will be denoted by $F_{K,\omega}$ and, using the notation $f = F^{-1}_{K,\omega}$ for the lift to the real line of the inverse of $F_{K,\omega}(x)$, the initial configuration can be written as

$$u^\alpha_n(0) = f(n\omega + \alpha), \tag{40}$$

where α is some constant. Once the potential is turned off, this configuration evolves asymptotically to some equispaced (integrable limit) configuration which we shall assume is reached at $t = \tau_{\rm off}$,

$$u^\alpha_n(\tau_{\rm off}) = n\omega + \beta. \tag{41}$$

Given α, the value of β is uniquely determined, due to Newton's third law which imposes that (on average) no net macroscopic motion occurs:

$$\langle u^\alpha_n(\tau_{\rm off}) - u^\alpha_n(0)\rangle = 0. \tag{42}$$

By decomposing $u_n^\alpha(0)$ as the sum of its integral and fractional parts, and using $\mathrm{Int}(u_n^\alpha(0)) = \mathrm{Int}(n\omega + \alpha)$ (recall that $F_{K,\omega}(0) = 0$ and $F_{K,\omega}(1) = 1$), equation (42) yields, for rational $\omega = p/q$ (p, q coprime),

$$\begin{aligned}\beta - \alpha &= q^{-1} \sum_{n=0}^{q-1} (\mathrm{Frac}(u_n^\alpha(0)) - \mathrm{Frac}(n\omega + \alpha)) \\ &= u_{cm}(K, \omega = p/q) - q^{-1}\mathrm{Frac}(q\alpha) - \frac{1}{2}(1 - q^{-1}),\end{aligned} \tag{43}$$

where $u_{cm}(K,\omega)$ denotes the d.f. (mod 1) centroid of the configuration $(u_n^\alpha(0))$. Note that the last equality follows from the expression for the distribution centroid in the period-q case, $u_{cm}(K, p/q) = q^{-1} \sum_{n=0}^{q-1} \mathrm{Frac}(u_n^\alpha(0))$, and from the solution to exercise 1 in section 4. For irrational values of ω the result is

$$\beta - \alpha = u_{cm}(K,\omega) - \frac{1}{2}. \tag{44}$$

From $0 \leq u_{cm} < 1$, one easily deduces that $|\beta - \alpha| \leq 1/2 + (2q)^{-1}$, and as[11] $\beta = \alpha$ whenever $q = 1$, we conclude that $|\beta - \alpha| \leq 3/4 < 1$ for all q. The consequence of this inequality is that not all particles pass over $u = 0$ (mod 1).

The absolute value of the partial local flow $|\mathcal{J}_{\mathrm{off}}^0|$ through $u = 0$ (mod 1) is the fraction $\mu(\alpha, \beta, \omega)$ of indices n such that $\mathrm{Int}(n\omega + \alpha) \neq \mathrm{Int}(n\omega + \beta)$. This quantity has been computed in exercise 2 of section 4 (36-37). Then the flow during the off-semicycle is $\mathcal{J}_{\mathrm{off}}^0 = \mathrm{sign}(\beta - \alpha)\mu(\alpha, \beta, \omega)$, which we can write as:

$$\mathcal{J}_{\mathrm{off}}^0 = \begin{cases} q^{-1}\mathrm{Int}\left(q\left(u_{cm}(K, p/q) - \frac{1}{2}(1 - q^{-1})\right)\right) & \text{for } \omega = p/q \\ u_{cm}(K,\omega) - \frac{1}{2} & \text{for irrational } \omega \end{cases} \tag{45}$$

Consider now the on-semicycle. At the beginning of this semicycle the initial configuration is equispaced, $u_n^\beta(0) = u_n^\alpha(\tau_{\mathrm{off}}) = n\omega + \beta$. Then this initial configuration evolves asymptotically to some recurrent RO equilibrium configuration which we assume is reached at $t = \tau_{\mathrm{on}}$, $u_n^\beta(\tau_{\mathrm{on}})$, a ground state for the parameter values K and ω. In order to compute the partial local flow $\mathcal{J}_{\mathrm{on}}^0$ through $u = 0$ (mod 1) during this semicycle, we have to introduce a quantity $\Delta(K,\omega)$, which we call the saddle phase.

Let us denote by M_m the set of values of δ for which $\mathrm{Int}(u_0^\delta(\tau_{\mathrm{on}})) = m$, with m integer, where $u_n^\delta(\tau_{\mathrm{on}})$ denotes the RO configuration of equispaced initial condition $u_n^\delta(0) = n\omega + \delta$. Using the property of order preservation of the dynamics, it is easily seen that if δ_1 and δ_2 are in M_m, then for all λ in $[0,1]$, $\lambda\delta_1 + (1 - \lambda)\delta_2$ is also in M_m. In other words, M_m is an interval. Moreover, the length of this interval is 1, because if δ is in M_m, then $\delta + 1$ is in M_{m+1}. We define the saddle phase Δ as the infimum of the interval M_0.

[11] Note that the ground states for integer values of ω are already equispaced.

If it is the case that the ground state equilibria corresponding to (K,ω) are pinned configurations, they are attracting fixed points of the dynamics, each one surrounded by its basin of attraction, the open set of initial configurations asymptotically evolving to the fixed point. The frontier of two contiguous basins contains an unstable equilibrium, a saddle (or minimax) configuration, which attracts only initial conditions on the frontier. On the other hand, the equispaced equilibria $(n\omega+\delta)$ of the system at $K=0$ form a line in the phase space, parametrized by δ. The intersection of the stable manifold of the saddle (*i.e.* the frontier) with the line of equispaced configurations is just $(u_n^{\Delta}(0))$. This geometrical interpretation justifies the term "saddle phase" for Δ. In a more physical language, the Peierls barrier (which is the energy of the saddle configuration relative to stable equilibria), produces the opening of a step (often called Peierls gap) in the distribution function (mod 1), which starts at Δ. If the equilibria are not pinned, then Δ corresponds to the phase of the initial configuration such that $u_0^{\Delta}(\tau_{\rm on})$ lies on top of a potential maximum. Though one cannot speak of a saddle in this case, we will keep the term for Δ.

Before computing the partial local flow $\mathcal{J}_{\rm on}^0$, we now prove that $|\Delta|<1$ (The following notation is used, $u_n^{\delta^+}=\lim_{\delta\to\delta^+}u_n^{\delta}$, and $u_n^{\delta^-}=\lim_{\delta\to\delta^-}u_n^{\delta}$). If it were the case that $\Delta\le -1$, then one could always find an RO equilibrium configuration $(\tilde u_n)$ with $\mathrm{Int}(\tilde u_0)=-1$ and $u_n^{\Delta^+}<\tilde u_n$ for all n (because the fluctuations of a RO configuration with respect to equispacing are strongly bounded - recall(17)). On one hand, as $(\tilde u_n)$ is an equilibrium configuration, $\tilde u_n(\tau_{\rm on})=\tilde u_n(0)$ for all n, so that $\mathrm{Int}(\tilde u_0(\tau_{\rm on}))=-1$; on the other hand, order preservation implies that $u_n^{\Delta^+}(\tau_{\rm on})\le\tilde u_n(\tau_{\rm on})$, so that $0=\mathrm{Int}(u_n^{\Delta^+}(\tau_{\rm on}))\le \mathrm{Int}(\tilde u_n(\tau_{\rm on}))=-1$. This contradiction proves that $\Delta>-1$. *Mutatis mutandi*, the same type of argument also proves that $\Delta<1$.

As the initial configuration is $u_n^{\beta}(0)=n\omega+\beta$, one easily realizes that the fraction of particles passing over $u=0$ (mod 1) during the on-semicycle is the fraction of indices n such that

$$\begin{aligned}\mathrm{Frac}(n\omega+\beta)<\Delta \qquad &\text{if } \Delta>0\\ \mathrm{Frac}(n\omega+\beta)\ge 1+\Delta \qquad &\text{if } \Delta\le 0\end{aligned} \tag{46}$$

that is, $\tilde F_{\omega,\beta}(\Delta)$ if $\Delta>0$, and $1-\tilde F_{\omega,\beta}(1+\Delta)$ if $\Delta>0$, where the d.f. (mod 1) $\tilde F_{\omega,\beta}(x)$ was computed in Exercise 1 of Section 4 (expressions (31) and (32)). Note that particles cross $u=0$ (mod 1) from right to left if $\Delta>0$ (negative flux) and from left to right if $\Delta<0$ (positive flux). Then using the expressions (43) and (44) for $\beta-\alpha$, we obtain

$$\mathcal{J}_{\rm on}^0=\begin{cases} q^{-1}\mathrm{Int}\left(-q\Delta+\mathrm{Frac}\left(q\left(u_{cm}-\frac{1}{2}(1-q^{-1})\right)\right)\right) & \text{for } \omega=p/q\\ -\Delta & \text{for irrational } \omega\end{cases} \tag{47}$$

(the same expressions for both signs of Δ).

Finally, the flow $\mathcal{J}(K,\omega)$ during the cycle is the sum of (45) and (47):

$$\mathcal{J}(K,\omega) = \begin{cases} \frac{1}{q}\,\mathrm{Int}\left(q\left(u_{\mathrm{cm}}(K,\frac{p}{q}) - \Delta(K,\frac{p}{q}) - \frac{1}{2}(1-\frac{1}{q})\right)\right) & \text{for } \omega = p/q \\ u_{\mathrm{cm}}(K,\omega) - \Delta(K,\omega) - \frac{1}{2} & \text{for irrational } \omega. \end{cases} \tag{48}$$

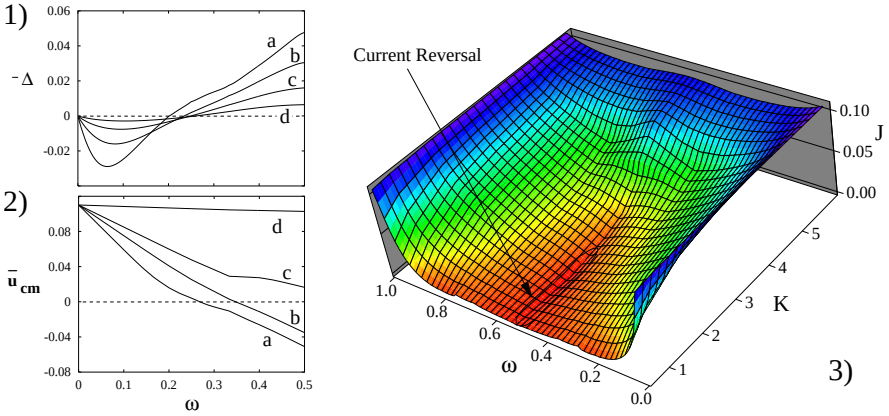

Fig. 4. Numerical results using the pinning potential $V(u) = (2\pi)^2[\sin(2\pi(u+b)) + 0.22\sin(4\pi(u+b))]$ with $b = 0.194969$. **(1)** shows the saddle phase $\Delta(K,\omega)$ for $K = 1, 2, 4, 10$ (labeled from a to d). The mean asymmetry $\overline{u}_{cm} = u_{cm} - 1/2$ is plotted in **(2)** for the same values of K. **(3)** shows the surface $\mathcal{J}(K,\omega)$ for $0.5 < K < 6.0$ and $0 < \omega < 1$. The figure reflects the crests of high flow near integer commensuration and the small region of current reversal around $\omega = 0.5$ at low values of K.

Both quantities, the distribution centroid $u_{cm}(K,\omega)$ and the saddle phase $\Delta(K,\omega)$, are continuous functions of K and ω: u_{cm} is a ground state average, and the Aubry-Mather theory assures that the ground state d.f. (mod 1) changes continuously. On the other hand, the saddle configuration also changes continuously, so that one expects the saddle stable manifold and consequently the saddle phase to vary continuously as well.

Thus, for the version 1 of the collective ratchet effect in the standard FK model, the flow is a well defined continuous function $\mathcal{J}(K,\omega)$ with point discontinuities at rational values of $\omega = p/q$; the size of these discontinuities behaves as $(2q)^{-1}$.

Given a particular potential function $V(u)$, the quantities $u_{cm}(K,\omega)$ and $\Delta(K,\omega)$ determining the flow can be computed with arbitrary numerical precision: The computation of u_{cm} only requires the obtention of the corresponding ground state configuration, which can be efficiently achieved by numerical integration of equation (38) for an equispaced initial configuration. Combining this with a simple bisection method provides also the value of Δ. Numerical results [26] of these quantities for an arbitrary chosen $V(u)$ are shown in figure 4(1) and 4(2). The resulting flow $\mathcal{J}(K,\omega)$ is shown in figure 4(3).

6.2 Switching interaction $W(\Delta u)$ on-off

We now consider the version 2 of the collective ratchet effect in the FK model. The initial configuration (before turning the coupling off) is a ground state $u_n^\alpha(0) = f(n\omega + \alpha)$. When the interaction $W(\Delta u)$ is switched off (anti-integrable limit), every single particle in the configuration evolves towards the minimum of its potential well, so that the asymptotic configuration is a recurrent stable RO uncoupled configuration, which can be written as

$$u_n^\alpha(\tau_{\rm off}) = {\rm Int}(n\omega + \alpha) + a. \tag{49}$$

Thus, during the off-semicycle, no particles pass over $u = 0 \pmod 1$, and the partial local flow $\mathcal{J}^0_{\rm off} = 0$.

Now the coupling parameter is turned on to the value C. It is easy to realize that for small enough values of C no particles can pass over a potential maximum. Indeed, if the coupling parameter is much smaller than the (absolute value of the) maximal slope of the pinning potential $V(u)$, the coupling forces cannot overcome the pinning forces and each particle will remain in its initial potential well, so that $\mathcal{J}^0_{\rm on} = 0$ for all ω.

In order to prove that there is a threshold value, likely dependent on the mean spacing ω, $C_{\rm th}(\omega) < \infty$, such that for $C > C_{\rm th}(\omega)$ the flow is non-zero, we can analyze the limit $C \to \infty$. This limit is equivalent to the limit $K \to \infty$ of the version 1; in this limit the distribution centroid u_{cm} of uncoupled configurations tends to a for all ω, and the saddle phase Δ tends to zero, so that from the equation (48) one obtains the limit flow

$$\mathcal{J}(\infty, \omega) = \begin{cases} q^{-1}{\rm Int}\left(q\left(a - \frac{1}{2}(1 - q^{-1})\right)\right) & \text{if } \omega = p/q \\ a - \frac{1}{2} & \text{if } \omega \text{ is irrational} \end{cases} \tag{50}$$

One concludes that, provided $a \neq 1/2$, the flow is zero only for those rationals $\omega = p/q$ such that $q \leq (2|a - 1/2|)^{-1}$, which is a finite set of values in the unit interval. Then, for each mean spacing ω (except at most a finite number of rationals per unit interval), there is a threshold value $0 < C_{\rm th}(\omega) < \infty$ of the coupling parameter separating two different regimes.

In order to visualize the existence of thresholds for transport, one can think of the phase portrait in configuration space: The recurrent stable RO equilibrium $u_n = f(n\omega + \alpha)$ has a basin of attraction whose frontier is the saddle stable manifold. For low values of C, the uncoupled configuration ${\rm Int}(n\omega + \alpha) + a$ belongs to this basin of attraction. Increasing the value of C results in a continuous variation of the ground state, the saddle, and the saddle stable manifold. When $C = C_{\rm th}(\omega)$ the saddle stable manifold touches on the point in configuration space representing the uncoupled configuration. A further increase of C places the uncoupled configuration inside the basin of attraction of the contiguous ground state.

We show in figure 5 the numerical computations [27] of $C_{\rm th}(\omega)$ for the same potential function $V(u)$ as in figure 4. One can clearly observe there both jump

and point discontinuities at rational values of ω. Note that $a \approx 0.610061$ and $(2|a-1/2|)^{-1} \approx 4.5$ for this potential, so C_{th}^{-1} could only be zero for $q \leq 4$, as confirmed by the numerics. Figure 6 shows numerical computations of the flow $\mathcal{J}(C,\omega)$ for some values of the coupling parameter C; the most remarkable aspect of these graphs is their piecewise linear shape. In the next section we will discuss these features from the perspective of the Discommensuration Theory.

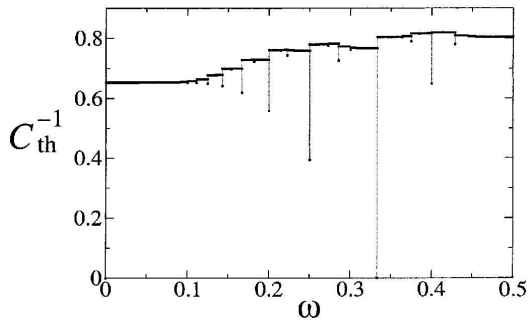

Fig. 5. Numerical computation of the inverse of the threshold coupling parameter (C_{th}^{-1}) as a function of ω (drop lines are guides for the eyes).

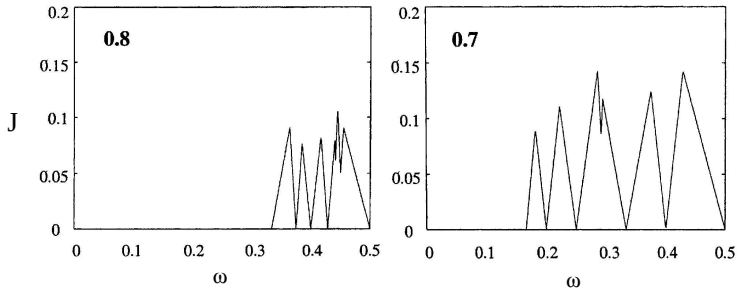

Fig. 6. Plot of the flow $\mathcal{J}(\omega)$ for two different values of the inverse coupling parameter $C^{-1} = 0.8$ and 0.7.

7 Discommensuration Theory

As mentioned in section 2, according to the Discommensuration (DC) Theory, a ground state of mean spacing ω, with phonon gap, is well approximated by

an "array of DCs" on a ground state of close enough rational mean spacing $\omega_0 = p/q$, more presisely, by a concatenation of segments of DCs of mean length $|q\omega - p|^{-1}$, with advanced DCs if $\omega > \omega_0$ and retarded DCs if $\omega < \omega_0$, the error being exponentially small in $|q\omega - p|$: at most $\exp(-1/(2\xi|q\omega - p|))$, where ξ is the decay range (coherence length) of the DC.

So provided ξc is small, where $c = |q\omega - p|$ is the density of DCs (inverse of the average spacing between DCs), the DCs in the array are almost non-interacting (thus almost identical) field excitations. This allows to describe the physical properties of the ground state of mean spacing ω in terms of the DC properties relative to the substrate configuration (the ground state of mean spacing ω_0).

A convenient variable for the representation of a DC is the averaged relative positions φ_j^{DC} of the DC configuration (w_j^{DC}) with respect to the substrate configuration $(u_j^{\omega_0})$:

$$\varphi_j^{\mathrm{DC}} = q^{-1} \sum_{i=0}^{q-1} \left(w_{j+i}^{\mathrm{DC}} - u_{j+i}^{\omega_0} \right) \tag{51}$$

Figure (7) illustrates the "intrinsic" properties of a DC: The *excess length* of a DC is the asymptotic difference $\lim_{j\to\infty} \varphi_j^{\mathrm{DC}} - \lim_{j\to-\infty} \varphi_j^{\mathrm{DC}} = \pm q^{-1}$, where $+$ is for advanced and $-$ for retarded DCs. The *width* of a DC is twice the decay range ξ of the substrate configuration, and the *center* of a DC is an index j_0 for which the deviation from the substrate configuration is maximum. A finite displacement of the DC center $j_0 \to j_0 + L$ involves a total displacement of particles $\approx \mp L q^{-1}$ relative to the substrate.

An array of identical DCs (on a substrate of mean spacing ω_0) with density (inverse number of particles between DC centers) $c = q|\omega - \omega_0| = |q\omega - p|$ has a d.f. (mod 1) F_ω as sketched in figure 7.c: there are new jumps (with respect to the substrate d.f. F_{ω_0}) located at the DC particle positions w_j^{DC} (mod 1), and the height of these jumps is the density c of the array. From these observations one can see that the F_ω-average of a period-1 test function g can be expressed as

$$\int_0^1 g \, dF_\omega = \int_0^1 g \, dF_{\omega_0} + c \, g^{\mathrm{DC}} \tag{52}$$

where the quantity g^{DC} is a characteristic (intrinsic property) of a single DC, thus independent of ω. The importance of equation (52) is that it provides the full Taylor (power) series expansion of macroscopic variables in a neighborhood of ω_0 (note that $c = q|\omega - \omega_0|$), which contains no terms higher than linear.

We will now derive explicitly equation (52) for the particular case $g(u) = \mathrm{Frac}(u)$, i.e. compute $u_{\mathrm{cm}}(\omega) - u_{\mathrm{cm}}(\omega_0)$ for values of ω very close to the rational ω_0:

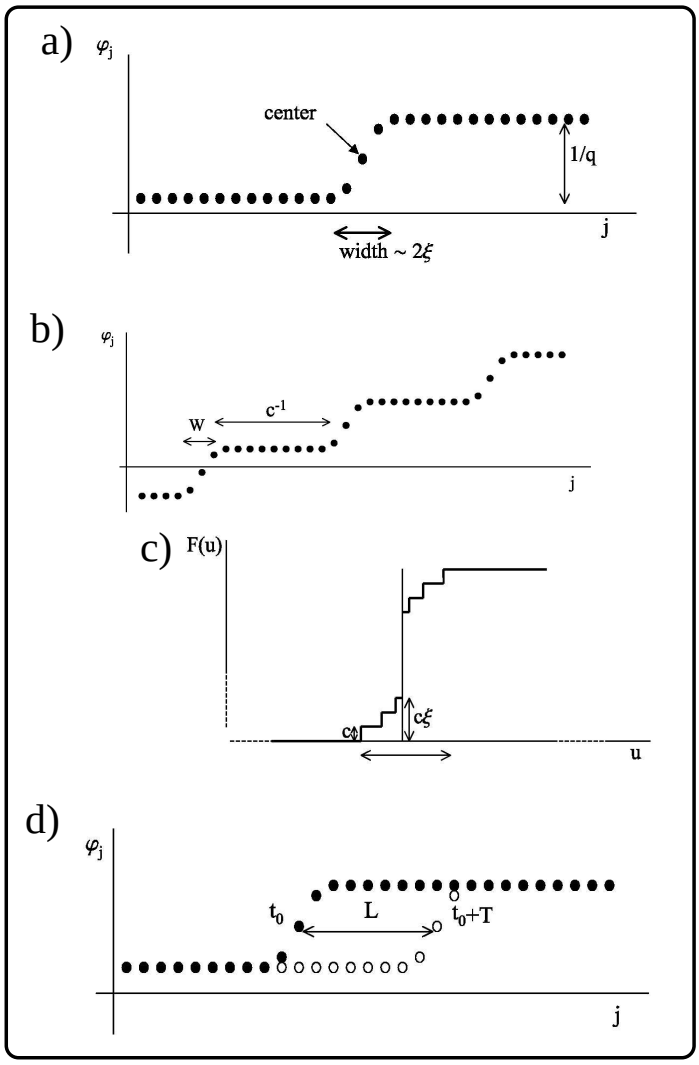

Fig. 7. **(a)** Graphical representation of the intrinsic properties of an advanced DC (see text for definitions). **(b)** Array of equispaced DCs. **(c)** Distribution function (mod 1) of an array of equispaced DCs over a commensurate configuration: each jump in the d.f. (mod 1) of the commensurate configuration (central vertical line in figure) is now splitted into several jumps at the DC particle positions, of heigth c. **(d)** The relative advance L of the DC center during a time T involves a microscopic total displacement of L/q relative to substrate.

$$u_{\rm cm}(\omega) - u_{\rm cm}(\omega_0) = \lim_{N\to\infty} (2N+1)^{-1} \sum_{n=-N}^{N} (\mathrm{Frac}(u_n^{\omega}) - \mathrm{Frac}(u_n^{\omega_0})) \quad (53)$$

$$\approx \lim_{N\to\infty} (2N+1)^{-1} \sum_{n=-N}^{N} (\mathrm{Frac}(v_n) - \mathrm{Frac}(u_n^{\omega_0})) \quad (54)$$

where (v_n) is the configuration of concatenated DCs, and an error of size at most $\exp(-1/(2\xi|q\omega - p|))$ is incured. Now, assuming $2N+1 \gg c^{-1} \gg 1$ we approximate the sum above as the number $c(2N+1)$ of DCs in the segment of length $2N+1$ times the average contribution of each DC. To make sense of the contribution $\sum_{n=-M}^{N}(\mathrm{Frac}(w_n^{\rm DC}) - \mathrm{Frac}(u_n^{\omega_0}))$ of a DC, where $w_n^{\rm DC}$ denote the particle positions in a DC configuration centered at $n=0$, one has to consider the limit of the sum over whole numbers of period q, $\lim_{k\to-\infty,l\to+\infty} \sum_{n=kq+i}^{lq+i}(\mathrm{Frac}(w_n^{\rm DC}) - \mathrm{Frac}(u_n^{\omega_0}))$, else in general it oscillates for ever as $M, N \to \infty$. This still depends on the phase $i \pmod q$, but it can be shown to cycle periodically through the q possibilities along the array of DCs. So the end result is that

$$\lim_{N\to\infty} (2N+1)^{-1} \sum_{n=-N}^{N} (\mathrm{Frac}(v_n) - \mathrm{Frac}(u_n^{\omega_0})) \approx c\,\alpha^{DC}\,, \quad (55)$$

with

$$\alpha^{DC} = \frac{1}{q} \sum_{i=1}^{q} \left(\sum_{k=-\infty}^{\infty} \left(\sum_{n=kq+i}^{kq+i+q-1} (w_n^{\rm DC} - u_n^{\omega_0}) \right) \right). \quad (56)$$

We can thus write, with exponentially small error:

$$u_{\rm cm}(\omega) = u_{\rm cm}(\omega_0) + |\omega - \omega_0| q \alpha^{\rm DC} \quad (57)$$

where $\alpha^{\rm DC}$ can be interpreted as the relative asymmetry of the DC with respect to the substrate ($\omega_0 = p/q$) configuration. In formula (57), it is to be understood that $\alpha^{\rm DC}$ must be computed with the advanced DC if $\omega > p/q$ and with the retarded one if $\omega < p/q$.

From equation (57), we see that whenever $\alpha^+ \neq -\alpha^-$ ($\pm$ denoting advanced/retarded DC), there is a jump discontinuity in the first derivative of $u_{\rm cm}(\omega)$. Unless some special symmetry is invoked in particular cases, these singularities must occur generically. Indeed, they are easily observed in the numerical computations [26] of the distribution centroid shown in figure 4.b. We also see clearly in figure 4.b that the saddle phase $\Delta(\omega)$ has a discontinuous first derivative. However this quantity is not a F_ω-average, so that the explanation of this observation cannot be made on the basis of (52) (note also that the very concept of DC looses all meaning in the integrable limit $K=0$).

As one should not expect that the discontinuities in the slope of $u_{\rm cm}(\omega)$ exactly cancel those of $\Delta(\omega)$, one concludes that the flow $\mathcal{J}(K,\omega)$ show discontinuous first partial derivative with respect to ω at rationals. Indeed, our numerical results are fully consistent with this expectation.

For the version 2 of the collective ratchet effect, the DC theory remains a valid approach during the complete cycle, provided C is bounded. An interesting consequence for the functional form of the flow dependence on ω is the following:

Assume that ω is close to a rational $\omega_0 = p/q$, $\omega > \omega_0$ (respectively $\omega < \omega_0$), and $C_{\rm th}(\omega) < C < \infty$. Let r^+ (resp. r^-) be the displacement of the advanced (resp. retarded) DC center relative to the substrate after a complete on-off cycle. (Note that, in general, r^+ and r^- can be different integers.) The flow $\mathcal{J}(C,\omega)$ can thus be written as

$$\begin{aligned} \mathcal{J}(C,\omega) &= \mathcal{J}(C,\omega_0) \mp r^{\pm}|\omega - \omega_0| \\ &= \mathcal{J}(C,\omega_0) - r^{\pm}(\omega - \omega_0) \end{aligned} \tag{58}$$

with exponentially small error. On one hand, this assures continuity of the flow respect to ω, and on the other a discontinuous first partial derivative whenever $r^+ \neq r^-$. The numerical computations of the flow shown in figure 6 confirm these expectations.

From the DC theory basic tenet, a DC configuration is the one-sided limit of a sequence of (commensurate or incommensurate) ground state configurations of average spacings ω_j approaching the rational p/q from the left (retarded DC) or right (advanced DC) side. Thus, the one-sided limit $C_{\rm th}((p/q)^{\pm})$ is the threshold coupling for the (advanced/retarded) DC configuration at $\omega = p/q$. Unlike the centroid, the threshold coupling is not a configuration average, and then there is no reason that $C_{\rm th}(p/q)$, $C_{\rm th}((p/q)^+)$ and $C_{\rm th}((p/q)^-)$ should coincide and they indeed do not, in general, as shown by numerical results in figure 5.

8 Exercises

1. A close inspection of the graph of $C_{\rm th}^{-1}(\omega)$ in figure 5 reveals that the value of $C_{\rm th}(\omega)$ at rationals is greater than its left-hand and right-hand limits there and, apart from these point discontinuities, $C_{\rm th}(\omega)$ is a step function. Use Discommensuration Theory to explain these numerical observations.

2. Metastable configurations of the FK model are stable configurations which are not m.e.c. They are assured to exist for all values of ω, provided K is high enough (or, equivalently, C is low enough). A simple type of metastable structure is an array of DCs on a commensurate substrate with a non-homogeneous interspacing between contiguous DCs. For the version 2 of the collective ratchet effect, an initial metastable configuration of this type can evolve after a complete on-off cycle into a translate of itself.
   (a) Give an argument supporting the previous statement.
   (b) Work out a numerical example confirming this assertion.

(c) Argue that this is not possible to happen for the version 1 of the collective ratchet effect.

3. Along these lecture notes we have assumed thermodynamic limit conditions. An important issue in some applications to experimental systems is how finite size effects can modify the system behaviour. Concerning dynamics, in particular, it is important to note that for finite chains the mean spacing ω is no longer a constant of motion. The parameter which controls the finite system length in the Standard model ($W(\Delta u) = \frac{1}{2}(\Delta u)^2 - \sigma \Delta u$) is the tension σ (*i.e.* the unstretched length of the "springs"). Also, the very notion of RO configuration is not so useful for a finite system. The aim of this exercise is to illustrate some of the differences in the behaviour in the version 1 of the ratchet collective effect. Consider an equispaced initial configuration of 720 particles with spacing 3/80, and integrate the equations of motion of overdamped dynamics at $K = 0.05$ for both periodic boundary conditions (pbc - infinite system size) and a finite system with $\sigma = 3/80$ with free boundary conditions (fbc).
(a) Compute the flow in both cases and plot the φ-profile:

$$\varphi_j = q^{-1} \sum_{i=0}^{q-1} (u_{j+i}^{\mathrm{fbc}} - u_{j+i}^{\mathrm{pbc}}) \tag{59}$$

(b) Explain the φ-profile and the difference in the flow in terms of the asymmetric entrance of DCs at boundaries.
(c) Answer question (a) for $K = 0.4$, and comment on the differences with respect to the case $K = 0.05$.

8.1 Solutions to Exercises

1. The positions (mod 1), $\mathrm{Frac}(w_j^{\mathrm{DC}})$, of the particles around the DC center j_0 are placed inside the gaps between the particle positions (mod 1) of the ground state configuration (see figure 7); in particular, there are particles in the DC configuration closer to the potential maxima. Then one expects that the threshold coupling of a DC is lower than the threshold of the commensurate substrate: $C_{\mathrm{th}}(p/q) > C_{\mathrm{th}}((p/q)^{\pm})$.
For the second observation, to fix ideas, consider an array of advanced DCs ($\omega >\sim p/q$) with a very low density $c = q\omega - p$, so that the DCs behave independently, *i.e.* each of them behaves as a single DC does. For $C < C_{\mathrm{th}}((p/q)^+)$ neither the DCs nor the substrate can move, then $C_{\mathrm{th}}(\omega) \geq C_{\mathrm{th}}((p/q)^+)$ for $\omega >\sim p/q$. On the other hand, as the DCs are assumed independent, they do move for $C > C_{\mathrm{th}}((p/q)^+)$, so that $C_{\mathrm{th}}(\omega) \leq C_{\mathrm{th}}((p/q)^+)$. Thus, provided the assumption of independent DCs holds, one concludes $C_{\mathrm{th}}(\omega) = C_{\mathrm{th}}((p/q)^+)$ for $\omega >\sim p/q$.

2. (a) Provided the distances between contiguous DCs in the array are large enough, each DC will move independently of the others for values of the coupling larger than the DC threshold. After a complete on-off cycle, the displacement of each DC center will be the same, then the distances between DCs will remain as the initial ones, and the final configuration will be a translate of the initial metastable configuration.

   (b) First, one has to compute a DC configuration on a commensurate ground state. We make the arbitrary choice $\omega_0 = 1/2$ and compute the advanced DC configuration by integrating the overdamped equations of motion (using a standard Runge-Kutta algorithm) for an initial equispaced configuration of 251 particles over 125 periods of $V(u)$. We use the same potential function as in the numerical examples shown in previous sections, and $C = 2$. Then, we construct the initial metastable structure by joining four finite pieces (of different length) of the DC configuration centered around the DC center and finally impose periodic boundary conditions (see figure 8).

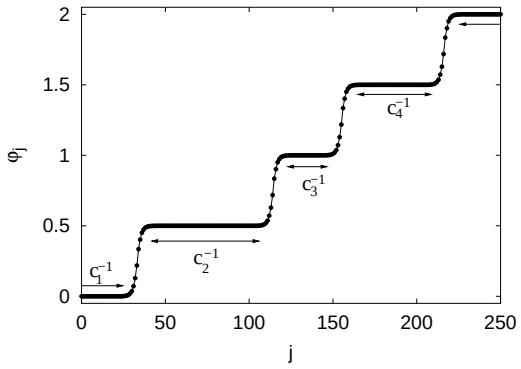

Fig. 8. Plot of φ_j for an array of 4 discommensurations. The substrate is an $\omega_0 = 1/2$ configuration, and $\omega = 21/40$. The coupling parameter is set to $C = 2$. The separation between the DCs (c_i^{-1}) in the metastable configuration are symbolized by the arrows between them.

After numerical integration of the equation of motion (during semicycle times large enough to assure that equilibrium is effectively reached after each semicycle), we observe that the final configuration is a translate of the initial one (see figure 9). As expected from the argument above, each DC center has been shifted by the same amount .

   (c) In the version 1 of the collective ratchet effect, any initial metastable configuration evolves asymptotically during the off-semicycle to an equispaced configuration. This cannot evolve back to metastable during the on-semicycle, so that the dynamical persistence of metastable configurations is impossible in version 1.

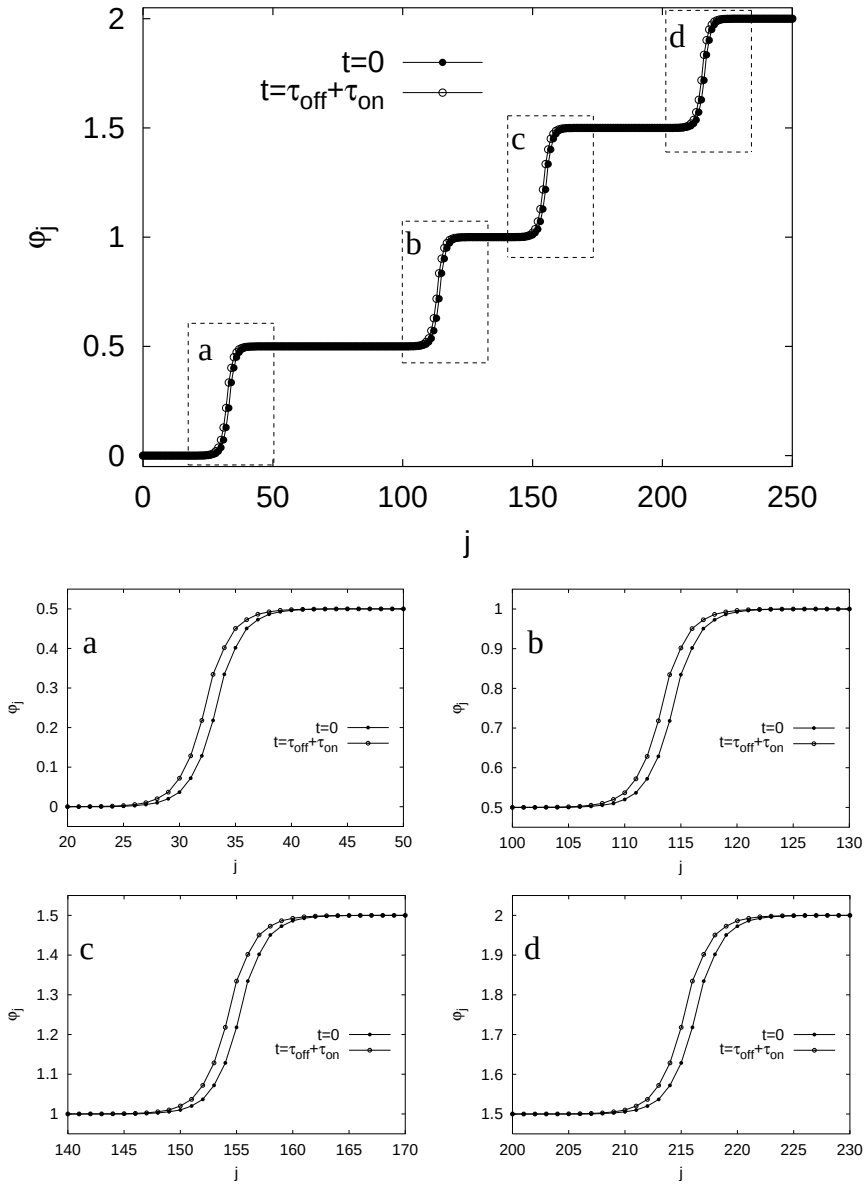

Fig. 9. Evolution of the metastable configuration of figure 8 after one period $\tau_{\rm off} + \tau_{\rm on}$. The initial distance between the DCs is preserved. As can be seen from the initial and final state of each DC (**(a)**, **(b)**, **(c)** and **(d)**) all the DCs centers have been shifted 1 site to the left.

3. (a) The results of the numerical computation of the φ-profile at different evolution times are plotted in figure (10). The flow difference is $0.12174 - 0.00589 = 0.11585$.
   (b) We observe a negative average slope of the φ-profile. Thus, the asymptotic equilibrium of the fbc configuration has a shorter total length than the pbc equilibrium; it can be described as an array of (equispaced) retarded DCs over the pbc configuration.
   The negative excess length (which for initial times is concentrated at the boundaries) spreads slowly over the whole chain. In other words, DCs enter on a short time scale, and then propagate on a larger time scale toward inner regions. One also observes that more DCs enter from the left boundary than from the right one, so that the center of mass of the final fbc configuration is displaced relative to that of the pbc one, explaining the flow difference. In figures (b) to (e) we plot the instantaneous force (or velocity) profile of the fbc chain.
   (c) For $K = 0.4$ the flow difference is much smaller: $0.04911 - 0.04653 = 0.00258$. As observed in the φ- profile in figure (11), the DCs that enter from the boundaries (due to the shortening of the chain length) are unable to overcome the Peierls-Nabarro barrier to their motion, and the negative excess length remains concentrated near boundaries. Consequently, inner regions of the chain do not feel any effect from the boundaries, and the macroscopic behaviour is unaffected by boundary conditions.

References

1. S.J. Gould *The Structure of Evolutionary Theory* (Harvard University Press, Cambridge 2002).
2. P.M. Chaikin and T.C. Lubensky *Principles of condensed matter physics* (Cambridge University Press, Cambridge 1995).
3. O.M. Braun and Yu. S. Kivshar, *The Frenkel-Kontorova model* (Springer, New York 2004).
4. D.K. Campbell, S. Flach, and Yu. S. Kivshar, *Phys. Tod.* **57**, 43 (2004).
5. S. Watanabe, H.S.J. van der Zant, S.H. Strogatz, and T. Orlando, *Physica D* **97**, 429 (1996).
6. F. Falo, P.J. Martínez, J.J. Mazo, T.P. Orlando, K. Segall and E. Trías, *Appl. Phys. A* **75**, 263 (2002).
7. M. Peyrard and A.R. Bishop, *Phys. Rev. Let.* **62**, 2755 (1989).
8. Th. Dauxois, M. Peyrard and A.R. Bishop *Phys. Rev. E* **47**, 684 (1993).
9. J.D. Weeks et al. arXiv:cond-mat/0406246v1 (2004).
10. M. Ridley *Evolution (second edition)* (Blackwell, Cambridge 1996).
11. S. Aubry and P.Y. Le Daeron, *Physica D* **8**, 381 (1983).
12. S. Aubry , in *Structures et Instabilitiés*, edited by C. Godréche (Les Ulis, France: Editions de Physique) 1985.
13. R.S. Mackay, Ph.D. thesis, Princeton University. Reprinted version in: R.S. Mackay, *Renormalisation in Area-preserving Maps*, (Singapore: World Scientific) 1993; *Physica D* **50**, 71 (1991).

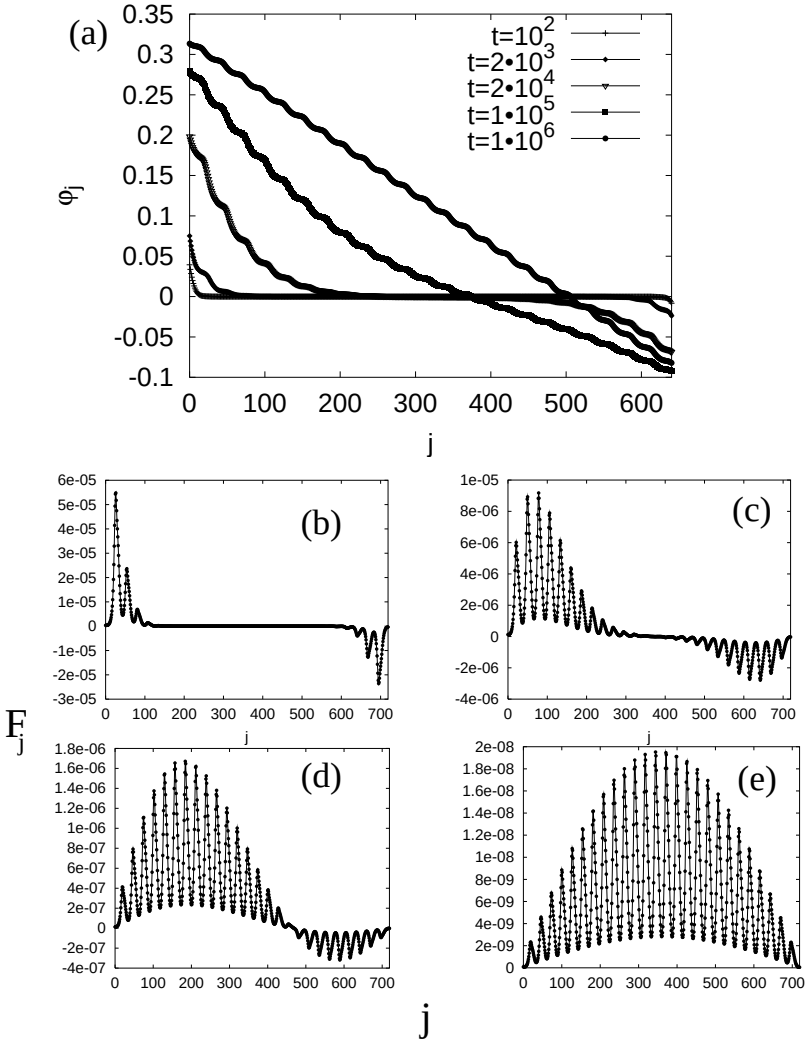

Fig. 10. **(a)** Time evolution of φ_j. The times of the instantaneous profiles are $t = 10^2$, $2 \cdot 10^3$, $2 \cdot 10^4$, 10^5 and $10^6 \simeq \tau_{relax}$. Figures **(b)**, **(c)**, **(d)** and **(e)** show the instantaneous force (or velocity) distribution of the fbc configuration at $t = 2 \cdot 10^3$, $2 \cdot 10^4$, 10^5 and 10^6 respectively.

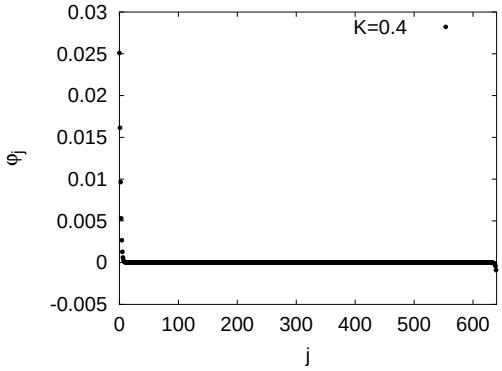

Fig. 11. Profile of φ_j for the $K = 0.4$ free ends configuration with $\sigma = 3/80$ and $N = 720$.

14. A. Scott, *Nonlinear Science: Emergence and Dynamics of Coherent Structures*, (Oxford: Oxford University Press) 1999.
15. A. Scott (editor), *Encyclopedia of Nonlinear Science*, (New York:Taylor and Francis) 2004.
16. C. Baesens, *Variational problems in solid state physics*, (unpublished) Lecture Notes (University of Warwick, 1994).
17. A. Katok and B Hasselblatt, *Introduction to the Modern Theory of Dynamical Systems* (Cambridge: CUP, 1995).
18. C. Golé, *Symplectic Twist Maps: Global Variational Techniques* (Advanced Series in Nonlinear Dynamics vol 18) (Singapore: World Scientific, 2001)
19. A.A. Middleton, *Phys. Rev. Lett.* **68**, 670 (1992).
20. L.M. Floría and J.J. Mazo, *Adv. Phys.* **45**, 505 (1996).
21. C. Baesens and R.S. Mackay, *Nonlinearity* **11**, 949 (1998).
22. C. Baesens and R.S. Mackay, *Nonlinearity* **17**, 949 (2004).
23. L. Kuipers and H. Niederreiter *Uniform distribution of sequences* (John Wiley and Sons, New York 1974).
24. *Appl. Phys A* **75** (2002), special issue on "Ratchets and Brownian motors", guest ed. H. Linke.
25. L.H. Tang, *Ph.D. Thesis*, (Carnegie-Mellon University 1987); L.H. Tang and R.B. Griffiths *J. Stat. Phys.* **53**, 853 (1988).
26. L. M. Floría, F. Falo, P.J. Martínez and J.J. Mazo, *Europhys. Lett.* **60**, 174 (2002).
27. L. M. Floría, P.J. Martínez, S. Flach and M.V. Fistul, *Physica D*, **187**, 100 (2004).

Index